

# Elastic properties of transition metal dioxides:

## $\text{XO}_2$ (X=Ru, Rh, Os, Ir)

Yanling Li<sup>1,2</sup>, Zhi Zeng<sup>2</sup>

*1. Department of physics, Xuzhou Normal University,*

*Xuzhou 221116, People's Republic of China*

*2. Key Laboratory of Materials Physics,*

*Institute of Solid State Physics, Chinese Academy of Sciences,*

*Hefei 230031, People's Republic of China and*

*Graduate School of the Chinese Academy of Sciences,*

*Beijing 100049, People's Republic of China*

(Dated: November 5, 2018)

### Abstract

The elastic properties of rutile transition metal dioxides  $\text{XO}_2$  (X=Ru, Rh, Os, and Ir) are investigated using first-principles calculations based on density functional theory. Elastic constants, bulk modulus, shear modulus, and Young's modulus as well as Poisson ratio are given.  $\text{OsO}_2$  and  $\text{IrO}_2$  show strong incompressibility. The hardness estimated for these dioxides shows that they are not superhard solids. The obtained Debye temperatures are comparative to those of transition metal dinitrides or diborides.

PACS numbers: 61.50.-f, 62.20.-x, 71.15.Mb, 71.20.-b, 77.74.Bw, 78.20.Ga

## I. INTRODUCTION

The rutile-type dioxides of transition metals (TMO<sub>2</sub>) possess a variety of electrical, mechanical, magnetic, and optical properties. It's electronic structure and electrical properties are widely studied due to their importance in technology. For example, OsO<sub>2</sub> and RuO<sub>2</sub> can be used as a possible electrode material in high-energy-density storage capacitors. Many of the TMO<sub>2</sub>s, such as RuO<sub>2</sub>, IrO<sub>2</sub> and TiO<sub>2</sub>, present a rich phase diagram. They can transform to other structures under high-pressure conditions. The first theoretical investigation on the electronic structures of the rutile transition metal dioxides (OsO<sub>2</sub>, IrO<sub>2</sub>, and RuO<sub>2</sub>), were reported by Mattheiss using a non-self-consistent augmented-plane-wave-linear-combinations-of-atomic orbitals method.[1] Subsequently, plenty of theoretical researches, including on the electronic, optical and structural properties were performed for rutile TMO<sub>2</sub>. Xu *et al* studied the electronic and optical properties of NbO<sub>2</sub>, RuO<sub>2</sub>, and IrO<sub>2</sub> using self-consistent calculations based on the linear muffin-tin-orbital method and atomic sphere approximation.[2] Krasovska *et al* calculated the optical and photoelectron properties of RuO<sub>2</sub> using the *ab initio* self-consistent energy-band structure.[3] Recently, the electronic and optical properties of RuO<sub>2</sub> and IrO<sub>2</sub> were reported by first-principles self-consistent electronic structure calculations based on the full-potential linearized plane wave method.[4]

In addition, the structural and mechanical properties of rutile transition metal dioxides have been widely investigated theoretically and experimentally. Structural phase transitions in IrO<sub>2</sub>[5] and RuO<sub>2</sub>[6] were reported based on first-principles calculations. Elastic properties of several potential superhard RuO<sub>2</sub> phases were studied by first-principles plane-wave pseudopotential and full-potential linearized augmented plane-wave methods.[7] Yen *et al* measured the first-order raman spectra of OsO<sub>2</sub> at room temperature.[8] Recently, the lattice dynamics of RuO<sub>2</sub> was given by theory and experiment.[9] However, to the best of our knowledge, few research on the elastic properties of IrO<sub>2</sub>, OsO<sub>2</sub> and RhO<sub>2</sub> has been reported so far.

In this paper, we focus on investigating the elastic properties of RuO<sub>2</sub>, RhO<sub>2</sub>, OsO<sub>2</sub> and IrO<sub>2</sub> using first-principles calculations based on density functional theory (DFT). Firstly, their structural parameters are optimized by first-principles total energy calculations. Secondly, the elastic constants are given by finite strain technique under the framework of linear response theory. Then the incompressibility of these TMO<sub>2</sub>s are discussed. Finally,

the hardness and Debye temperature are estimated.

## II. COMPUTATIONAL DETAILS

All calculations are performed by the CASTEP code using *ab initio* pseudopotentials based on DFT. For the exchange-correlation functional the generalized gradient approximation (GGA), as given by Perdew, Becke, and Ernzerhof (PBE), is applied. All the possible structures are optimized by the BFGS algorithm which provides a fast way of finding the lowest energy structure and supports cell optimization. In the calculation, the interaction between the ions and the electrons is described by using Vanderbilt's supersoft pseudopotential with the cutoff energy of 380 eV. The Monkhorst-Pack  $\mathbf{k}$ -point grid with a fine quality Brillouin zone sampling of  $2\pi \times 0.04 \text{ \AA}^{-1}$  is used in the calculations. In the geometrical optimization, all forces on atoms are converged to less than  $0.002 \text{ eV/\AA}$ , all the stress components are less than 0.02 GPa, and the tolerance in self-consistent field (SCF) calculation is  $5.0 \times 10^{-7} \text{ eV/atom}$ . The relaxation of the internal degrees of freedom is allowed at each unit cell compression or expansion. The elastic constants of  $\text{TMO}_2$  are obtained by using the finite strain technique. From the full elastic constant tensor we determine the bulk modulus  $B$ , the shear modulus  $G$ , the Young's modulus,  $E$ , and Poisson's ratio  $\nu$  according to the Voigt-Reuss-Hill (VRH) approximation.[10]

## III. RESULTS AND DISCUSSIONS

The tetragonal rutile structure belongs to space group  $P42/mnm$ . There are six atoms per unit cell. Two metal atoms locate at  $(0, 0, 0)$  sites and four oxygen atoms position at  $(u, u, 0)$  sites, where  $u$  is the internal parameter. The metal atoms are surrounded by six oxygen atoms at the corners of a slightly distorted octahedron, while the three metal atoms coordinating each of the oxygen atoms lie in a plane at the corners of a nearly equilateral triangle. Equilibrium volumes, crystal constants, and internal parameters are shown in Table I. It can be seen that all the structural parameters optimized here agree well with previous results. We find that there are very slight differences in volume and internal parameter ( $u$ ) between  $\text{TMO}_2$ s studied.

The calculated elastic constants  $c_{ij}$  are given in Table II. It is easy to see that these

constants  $c_{ij}$  satisfy the Born-Huang stability criteria,

$$\begin{aligned} c_{ii} > 0 (i = 1, 3, 4, 6), c_{11} > c_{12}, \\ c_{11} + c_{33} > 2c_{13}, 2c_{11} + c_{33} + 2c_{12} + 4c_{13} > 0, \end{aligned} \quad (1)$$

suggesting that they are mechanically stable. From the elastic constants calculated above, we obtain the bulk modulus  $B$ , shear modulus  $G$ , Young's modulus  $E$ , and Poisson's ratio  $\nu$  and list them in Table II, which are important to understand the elastic properties of TMO<sub>2</sub>s. For RuO<sub>2</sub>, our results agree well with the available theoretical and experimental values, indicating that PBE-GGA can be used to calculate the elastic properties of TMO<sub>2</sub>. OsO<sub>2</sub> and IrO<sub>2</sub> have the close bulk moduli and Young's moduli, which are higher than those of RuO<sub>2</sub> and RhO<sub>2</sub>. Higher bulk modulus indicates strong incompressibility. From Table II, we conclude that IrO<sub>2</sub> and OsO<sub>2</sub> are more difficult to be compressed than the two others, meaning that IrO<sub>2</sub> and OsO<sub>2</sub> are hard solids. The incompressibility of these TMO<sub>2</sub> can also be seen from relative volume as a function of pressure (Fig. 1). While there isn't a large difference in the shear modulus at four TMO<sub>2</sub>s, it's roughly the same. Also we note that there are few difference (13 GPa at most) between  $c_{44}$  and shear modulus  $G$  for four dioxides.

Employing the correlation between the shear modulus and Vickers hardness reported by Teter [12], the hardness of four TMO<sub>2</sub>s is estimated. By using the calculated  $G$  values reported in Table II and the correlation given by Teter we find a theoretical Vickers hardness of approximately 14.1 GPa for RuO<sub>2</sub>, 12.3 GPa for RhO<sub>2</sub>, 14.8 GPa for OsO<sub>2</sub> and 14.6 GPa for IrO<sub>2</sub>. It is well known that the hardness of superhard materials should be higher than 40 GPa, so that TMO<sub>2</sub> are not superhard materials.

Poisson's ratio reflects the stability of a crystal against shear. This ratio can formally take values between -1 and 0.5, which corresponds respectively to the lower limit where the material does not change its shape, and to the upper limit when the volume remains unchanged. All the calculated Poisson's ratios (Table II) are bigger than 0.25, which means that there are strong elastic anisotropy in these TMO<sub>2</sub>. In order to predict the brittle and ductile behavior of solids, Pugh introduced the ratio of the bulk modulus to shear modulus of polycrystalline phases. A high (low)  $B/G$  value is associated with ductility (brittleness). The critical value which separates ductile and brittle materials is about 1.75. The bigger difference obtained between bulk and shear modulus indicates higher ductility of these TMO<sub>2</sub>

(Table II).

Now, we discuss the elastic anisotropy of  $\text{TMO}_2$ . For the rutile structure, the directional bulk modulus along crystallographic axis and the percent elastic anisotropy defined by Chung and Buessem are discussed (Table III). From Table III, it can be seen that the directional bulk modulus is larger along the  $c$  axis than that along the  $a(b)$  axis, indicating that the incompressibility along the  $c$  axis is stronger than that along the  $a(b)$  axis. This anisotropy of compression along different lattice axis can be clearly seen from the increasing fractional axis compression  $c/a$  versus pressure (Fig. 2). On the other hand, the percentage of elastic anisotropy involves both the percentage anisotropy in compressibility  $A_B$  and in shear  $A_G$ . A value of zero represents elastic isotropy and a value of 1 (100%) is the largest possible anisotropy. The calculated  $A_B$  and  $A_G$  are listed in Table III. Obviously, these  $\text{TMO}_2$ s possess strong shear anisotropy and weak bulk anisotropy.

Further, the Debye temperature  $\Theta_D$  is also discussed because the Debye temperature relates to many physical properties of materials, such as specific heat, dynamical properties, and melting temperature. It can be calculated from the average wave velocity  $v_m$  by the equation[13]

$$\Theta_D = \frac{h}{k} \left[ \frac{3n}{4\pi} \left( \frac{\rho N_A}{M} \right) \right]^{1/3} v_m \quad (2)$$

where  $h$  is Plank's constant,  $k$  is Boltzmann's constant,  $N_A$  is Avogadro's number,  $\rho$  is density,  $M$  is molecular weight and  $n$  is the number of atom in the molecule.  $v_m$  is approximately given by

$$v_m = \left[ \frac{1}{3} \left( \frac{2}{v_t^3} + \frac{1}{v_l^3} \right) \right]^{-1/3} \quad (3)$$

where  $v_l$  and  $v_t$  are the transverse and longitudinal elastic wave velocity of the polycrystalline material and are given by Navier's equation[14]

$$v_t = \left( \frac{G}{\rho} \right)^{1/2} \quad (4)$$

and

$$v_l = \left( \frac{B + \frac{4G}{3}}{\rho} \right)^{1/2} . \quad (5)$$

The calculated density, longitudinal, transverse, and average elastic velocities and Debye temperatures  $\Theta_D$  for four  $\text{TMO}_2$ s are given in Table IV. Debye temperatures  $\Theta_D$  of  $\text{RuO}_2$  is comparative to the value of 866.4  $K$  in  $\text{ReB}_2$ [15] and ones of  $\text{OsO}_2$  and  $\text{IrO}_2$  is comparative to the value of 691  $K$  in  $\text{OsN}_2$ . [16]

## IV. CONCLUSION

In summary, the elastic properties of transition metal dioxides with rutile structure are investigated using first-principles calculations under the framework of density functional theory within generalized gradient density approximation. Elastic constants, bulk modulus, shear modulus, and Poisson's ratio are given. OsO<sub>2</sub> and IrO<sub>2</sub> have stronger incompressibility than RuO<sub>2</sub> and RhO<sub>2</sub>. The estimated hardness is 14.1 GPa for RuO<sub>2</sub>, 12.3 GPa for RhO<sub>2</sub>, 14.8 GPa for OsO<sub>2</sub> and 14.6 GPa for IrO<sub>2</sub>, which show that these dioxides are not superhard solids. Debye temperatures calculated by elastic constants and density are 846 K, 795 K, 674 K, 674 K for RuO<sub>2</sub>, RhO<sub>2</sub>, OsO<sub>2</sub>, and IrO<sub>2</sub>, respectively.

## V. ACKNOWLEDGEMENT

This work was supported by the National Science Foundation of China under Grant Nos 10504036 and 90503005, the special Funds for Major State Basic Research Project of China(973) under grant no. 2005CB623603, Knowledge Innovation Program of Chinese Academy of Sciences, and Director Grants of CASHIPS. Part of the calculations were performed in the Shanghai Supercomputer Center.

- 
- [1] L. F. Mattheiss, Phys. Rev. B **13**, 2433 (1976).
  - [2] J. H. Xu, T. Jarlborg, and A. J. Freeman, Phys. Rev. B **40**, 7939 (1989).
  - [3] O. V. Krasovska, E. E. Krasovskii, and V. N. Antonov, Phys. Rev. B **52**, 11825 (1995).
  - [4] J. S. de Almeida and R. Ahuja, Phys. Rev. B **73**, 165102 (2006).
  - [5] S. Ono, J. P. Brodholt, and G. D. Price, J. Phys.: Condens. Matter **20**, 045202 (2008).
  - [6] H. W. Hugosson, G. E. Grechnev, R. Ahuja, U. Helmerson, L. Sa, and O. Eriksson, Phys. Rev. B **66**, 174111 (2002).
  - [7] J. S. Tse, D. D. Klug, K. Uehara, and Z. Q. Li, Phys. Rev. B **61**, 10029 (2000).
  - [8] P. C. Yen, R. S. Chen, Y. S. Huang, C. T. Chia, R. H. Chen, and K. K. Tiong, J. Phys.: Condens. Matter **15**, 1487 (2003).
  - [9] K. -P. Bohnen, et al, Phys. Rev. B **75**, 092301 (2007).

- [10] R. Hill, Proc.Phys.Soc.London **65**, 349 (1952).
- [11] R. M. Hazen and L. W. Finger, J. Phys. Chem. Solids **42**, 143 (1981).
- [12] D. M. Teter, MRS. Bull. **23**, 22 (1998).
- [13] O. L. Anderson, J. Phys.Chem. Solids **24**, 909 (1963).
- [14] E. Schreiber, O. L. Anderson, and N. Soga, Elastic Constants and their Measurements (McGraw-Hill, New York, 1973).
- [15] X. Hao, Y. Xu, Z. Wu, D. Zhou, X. Liu, X. Cao, and J. Meng, Phys.Rev.B **74**, 224112 (2006).
- [16] Z. Wu, X. Hao, X. Liu, and J. Meng, Phys.Rev.B **75**, 054115 (2007).

## FIGURE CAPTIONS

**Fig.1:**  $V/V_0$  as a function of pressure for seven TMO<sub>2</sub>.

**Fig.2:**  $c/a$  ratio as a function of pressure for seven TMO<sub>2</sub>.



## TABLE CAPTIONS

**TABLE I:** Equilibrium lattice parameters,  $V_0(\text{\AA}^3)$ ,  $a$  ( $\text{\AA}$ ),  $c$  ( $\text{\AA}$ ), density  $\rho$  ( $\text{g/cm}^3$ ), and internal parameter  $u$  along with the available experimental values.

**TABLE II:** Zero-pressure elastic constants  $c_{ij}$  (GPa), the isotropic bulk modulus  $B$  (GPa), shear modulus  $G$  (GPa), Young's modulus  $E$  (GPa) and Poisson's ratio  $\nu$ .

**TABLE III:** The bulk modulus along the crystallographic axes  $a$ , and  $c$  ( $B_a$  and  $B_c$ ) for  $\text{TMO}_2$ . Percent elastic anisotropy for shear and bulk moduli  $A_G$  (in %),  $A_B$  (in %) and compressibility anisotropy factors  $A_{B_a}$  and  $A_{B_c}$ . Here,  $A_{B_a} = \frac{B_a}{B_b} = 1$ ,  $A_{B_c} = \frac{B_c}{B_b}$ .

**TABLE IV:** The longitudinal, transverse, average elastic wave velocity ( $v_l$ ,  $v_t$ , and  $v_m$  in  $m/s$ ), and Debye temperature  $\Theta_D$  ( $K$ ) at the theoretical equilibrium volume.

TABLE I: Li *et al.*

	$V_0$	$a$	$c$	$u$	Reference
RuO <sub>2</sub>	63.1488	4.5076	3.1080	0.3055	This
		4.4919	3.1066	0.306	[1]
RhO <sub>2</sub>	66.7652	4.6051	3.1482	0.3067	This
OsO <sub>2</sub>	64.3639	4.4943	3.1865	0.3078	This
		4.5003	3.1839	0.308	[1]
IrO <sub>2</sub>	67.4532	4.5899	3.2018	0.3082	This
		4.4983	3.1544	0.307	[1]
	65.79	4.541	3.191	0.3085	[5]

TABLE II: Li *et al.*

	$c_{11}$	$c_{33}$	$c_{44}$	$c_{66}$	$c_{12}$	$c_{13}$	$B$	$G$	$E$	$\nu$	Ref.
RuO <sub>2</sub>	303	536	117	221	240	190	260	104	275	0.3239	This
	299	558	114	227	246	199	258				[9]
							270				[11]
RhO <sub>2</sub>	268	498	103	190	216	166	232	91	242	0.3263	This
OsO <sub>2</sub>	337	631	109	243	270	210	292	109	291	0.3338	This
IrO <sub>2</sub>	344	605	117	219	274	223	299	108	290	0.3381	This

TABLE III: Li *et al.*

	$B_a$	$B_c$	$A_{B_c}$	$A_B$	$A_G$
RuO <sub>2</sub>	633	1339	2.1155	1.66	21.01
RhO <sub>2</sub>	560	1219	2.1751	1.89	22.24
OsO <sub>2</sub>	700	1573	2.2458	2.02	21.93
IrO <sub>2</sub>	718	1600	2.2284	1.76	18.83

TABLE IV: Li *et al.*

	$\rho$	$v_l$	$v_t$	$v_m$	$\Theta_D$
RuO <sub>2</sub>	6.9995	7548	3852	4316	846
RhO <sub>2</sub>	6.7117	7261	3687	4133	795
OsO <sub>2</sub>	11.4687	6180	3086	3463	674
IrO <sub>2</sub>	11.0413	6334	3133	3516	674

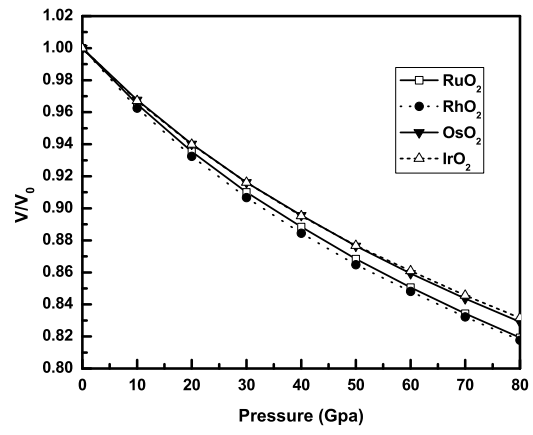


FIG. 1: Li *et al.*

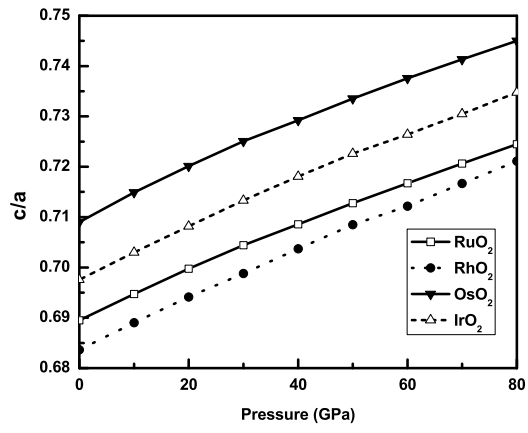


FIG. 2: Li *et al.*